Journal of Materials Chemistry C

Accepted Manuscript

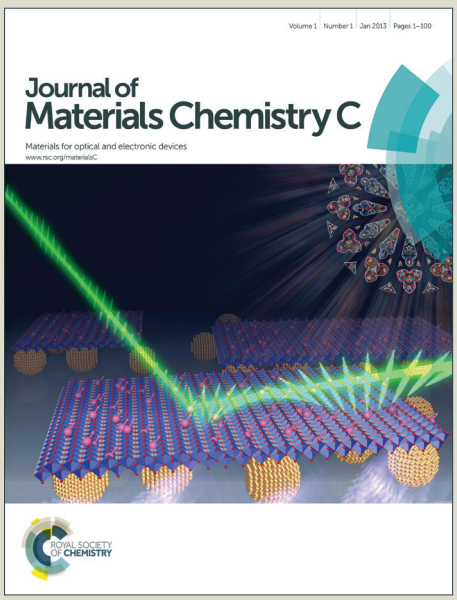

ROYAL SOCIETY OF CHEMISTRY

www.rsc.org/materialsC

Two-Component Solution Processing of Oxide Semiconductors for Thin-Film Transistors *via* Self-Combustion Reaction

Young Hun Kang,‡ Sunho Jeong,‡ Jung Min Ko, Ji-Yoon Lee, Youngmin Choi,

Changjin Lee,* and Song Yun Cho*

Division of Advanced Materials, Korea Research Institute of Chemical Technology, 141 Gajeong-ro, Yuseong-gu, Daejeon 305-600, Republic of Korea. E-mail: scho@krict.re.kr; Fax: +82 42-860-7200; Tel: +82 42-760-7260

†Electronic supplementary information (ESI) available: XPS spectra, AFM and SEM images, XRD patterns, thermal analysis, and transfer and output characteristics are available. Fig. S1-S15.

‡ Young Hun Kang and Sunho Jeong contributed equally to this work.

Indium zinc oxide (IZO) thin films were fabricated *via* self-combustion of In and Zn salts coordinated with fuel and oxidizer ligands. The intense heat generated from the exothermic reaction compensated for the energy required for oxide formation and reduced the temperature required to anneal the oxide films. Thermal analysis of the fuel and oxidizer precursors confirmed the generation of exothermic heat at a relatively low annealing temperature. With the aid of the internal energy that evolved as heat from the combustion reaction, the formation of the metal–oxygen–metal lattice and the removal of organic ligands could be easily accomplished with lower amounts of externally supplied energy. IZO thin-film transistors (TFTs), obtained from this combustive In–Zn pair at a low annealing temperature of 350 °C, showed a significantly enhanced field-effect mobility of 13.8 $cm^2 V^{-1} s^{-1}$ and a high on/off current ratio of 1.06×10^8. Inkjet printing of the combustive precursors yielded TFTs with a high field-effect mobility of 5.3 $cm^2 V^{-1} s^{-1}$ and an on/off ratio of 10^6. The high performance, good device uniformity, and high yield of TFTs fabricated by our self-combustion method demonstrate the potential of the proposed system to facilitate the processing of flexible printed electronics.

1. Introduction

Amorphous metal oxide thin-film transistors (TFTs), widely used in electronics, have several advantages such as high electrical performance and good device uniformity. Their disadvantages include high cost of processing equipment and facilities, which is typical of vacuum-based techniques such as pulsed laser deposition, atomic layer deposition, chemical vapor deposition, and radio-frequency magnetron sputtering.[1-4] Solution-phase techniques, on the other hand, feature easy control of material composition, large-scale deposition, high throughput, and low cost.[5-9] Challenges in developing solution-processed metal oxide TFTs include finding easily-processable materials, and effecting the hydrolysis, condensation, densification, and complete decomposition of organic ligands at low annealing temperatures. In the absence of high-temperature annealing, organic ligands (e.g., nitrides, halides, acetates) can remain in the metal oxide thin film, and the conversion of the oxide precursor can be incomplete, which might result in lower carrier mobility and adversely affect the TFT subthreshold slope as well as the on/off current and switching voltage.

Recently, new approaches have been investigated to produce low-temperature, solution-processed metal oxide TFTs from indium oxide, indium zinc oxide (IZO), indium gallium zinc oxide (IGZO), yttrium indium oxide (YIO), and indium zinc tin oxide (IZTO).[10-15] Chang and co-workers reported a high mobility of 11.8 $cm^2 V^{-1} s^{-1}$ in indium oxide TFTs annealed at 250 °C *via* an O_2/O_3 atmospheric process.[16] Sirringhaus and co-workers accomplished a mobility of ~10 $cm^2 V^{-1} s^{-1}$ in IZO and IGZO TFTs at 275 °C using moisture-sensitive alkoxide precursors; the films had to be prepared in a glove box for reproducibility, and annealed under a humid atmosphere to activate the metal oxide conversion reaction within the precursor films.[17] Park and co-workers fabricated IZO and IGZO TFTs with a mobility of ~10

$cm^2 V^{-1} s^{-1}$ on aluminum oxide gate insulators, *via* photochemical reactions activated by deep ultraviolet irradiation in a nitrogen atmosphere.[18] However, to achieve good device performance, these approaches required additional photo/chemical post-treatment to produce the desired oxide semiconductor skeletons for TFT applications. In contrast, recently developed chemical methodologies based on combustion reactions have facilitated the fabrication of high performance soluble oxide semiconductors simply by using the conventional annealing process.[19,20] The combustion reaction supplies heat to the precursor films, dramatically lowering the annealing temperature down to 300 °C while achieving mobility as high as 6.5 $cm^2 V^{-1} s^{-1}$. A drawback to this novel methodology is the effort involved in finely adjusting the chemical composition of the metal precursors, fuel, oxidizer, and additives to induce an exothermic reaction that generates sufficient heat.[21-27]

In the present study, a chemical combustion pathway using self-combustion is described, and the obtained results are compared with those of previously discussed chemical methodologies for the low-temperature synthesis of metal oxide TFTs. The conventional combustion system, which includes addition of external fuels and oxidizers, is an incredibly sensitive process. Even minor deviation from the exact amount of fuel, oxidizer, or pH controller required can result in malfunction of the TFTs. The fundamental issue of our study is the preparation of a stable and reproducible precursor solution for a TFT by means of "self"-combustion chemistry. Our facile, efficient self-combustion process overcomes the shortcomings of conventional combustive approaches by simply blending two metal precursors that contain coordinated fuel and oxidizer ligands. In the fabrication of soluble oxide TFTs for optoelectronic devices, the pivotal issue is the preparation of a *stable* and *reproducible* precursor solution. We demonstrate the combustion of the precursors without

additional fuels, oxidizers, or other components. This simple precursor solution results in more stable and uniform TFT devices owing to its easily controllable composition and facile activation, for the production of high performance soluble oxide semiconductors. We report here our initial results regarding the role of the exothermic self-combustion process and the chemistry of metal precursor (fuel–oxidizer) pairings in enhancing the characteristics of TFTs. The performance of TFTs is discussed as a function of the precursor composition and the annealing temperature. Finally, the fabrication of oxide TFTs *via* inkjet printing of the self-combustive precursor solution will be addressed.

2. Results and discussion

Terminology: The following terminology is used in this publication to describe the pair of In–Zn precursors. The precursor solution consisting of $Zn(C_5H_7O_2)_2{\cdot}xH_2O$ (Zn_{AC}) and $In(NO_3)_3{\cdot}xH_2O$ (In_{NO}) is denoted as $I_{NO}Z_{AC}O$. The precursor solution of $Zn(C_5H_7O_2)_2{\cdot}xH_2O$ and $In(C_5H_7O_2)_3{\cdot}xH_2O$ (In_{AC}) is $I_{AC}Z_{AC}O$. The precursor solution of $Zn(NO_3)_2{\cdot}6H_2O$ (Zn_{NO}) and $In(NO_3)_3{\cdot}xH_2O$ and that of $ZnCl_2$(Zn_{Cl}) and $InCl_3$(In_{Cl}) are denoted as $I_{NO}Z_{NO}O$ and $I_{Cl}Z_{Cl}O$, respectively.

The combustion reaction between organic fuels (e.g., acetylacetone, urea, carbohydrazide, citric acid) and oxidizers (e.g., nitrate), can lower the effective annealing temperature for the formation of metal oxide compounds from oxide precursors.[23,24] When a fuel–oxidizer pair is moderately heated, a highly intense exothermic reaction occurs. The evolved heat can accelerate the transformation of metal hydroxides or alkoxides into the corresponding metal oxide frameworks at sufficiently low external temperatures. Previous studies have

demonstrated that the combination of metal nitrates (as both a metal source and oxidizer) and acetylacetone (AcAc, as both a chelating agent and fuel) is most effective, among the various oxidizers and fuels, in generating high performance oxide semiconductors.[23,24]

As a representative material system for the chemical combustion-based synthesis, we studied indium gallium oxide (IGO), for which a mixture of indium nitrate hydrate and gallium nitrate hydrate was used as an oxidizer, and AcAc was used as a fuel. First, the electrical characteristics of fuel-free IGO TFTs were investigated in order to determine the most adequate chemical composition of In and Ga (Supplementary Information Fig. S1†). Taking into consideration all device parameters, including field-effect mobility, threshold voltage, off current, and subthreshold swing, an IGO composition with an In/Ga molar ratio of 7:3 was chosen. The mobility was 1.0 $cm^2 V^{-1} s^{-1}$ when the IGO channel layer was annealed at 300 °C. As expected, when the AcAc fuel was incorporated, with NH_4OH to control the pH, the device performance dramatically improved. The field-effect mobilities of IGO TFTs depended on the AcAc composition (R_1 value of 1 to 3) and NH_4OH composition (R_2 value of 1 to 4), summarized in Supplementary Information Table S1. R_1 indicates the molar ratio of AcAc to the metal salts and R_2 indicates the molar ratio of water molecule in an ammonium hydroxide (NH_4OH) solution to metal salts, respectively. When the IGO channel layers were annealed at 300 °C, their highest average field-effect mobility was 12.5 $cm^2 V^{-1} s^{-1}$, which is higher than that of the previously reported, combustion-derived In_2O_3, IZO, ZTO, and YIO TFTs. Interestingly, even with an annealing temperature as low as 250 °C, the device was still active with a field-effect mobility of 2.45 $cm^2 V^{-1} s^{-1}$. This indicates that IGO framework can indeed be formed *via* combustion chemistry, and the IGO precursor solutions were of the appropriate composition. However, as shown in Fig. 1(a) and (b), among the 11 synthetic

conditions, high performance was only achieved when AcAc and NH_4OH were incorporated at $R_1 = 1$ and $R_2 = 3$, respectively. For most synthetic conditions, the field-effect mobilities were below 5 $cm^2 V^{-1} s^{-1}$ and 1 $cm^2 V^{-1} s^{-1}$ for IGO TFTs annealed at 300 and 250 °C, respectively. Of greater concern was the bimodal distribution of field-effect mobility, shown in Fig. 1(c), observed even under the optimized synthetic conditions, upon testing 33 devices. Fig. 1(d) shows the transfer characteristics of a representative TFT. This result implies that it is nearly impossible to obtain stable and reproducible TFTs through a multiple-component-based combustion reaction. In this study, the preparation of the IGO precursor solution was carried out in an Ar-filled glove box to avoid the undesirable incorporation of water, which can limit the fabrication of large area TFTs.

This statistical data establishes that the formation of oxide frameworks by chemical combustion is significantly influenced by the chemical composition of the precursor mixture and complicated chemical reactions of each component, which should be well-controlled to ensure reproducibility and high performance in the resulting devices. To ensure sufficient exothermic heat, the chemical environment around the metal precursors should be adjusted by adding the proper amount of acid or base, in addition to optimizing the relative composition of oxidizer and fuel. In metal-salt-based chemistries, metal cations are solvated by water molecules, which are supplied in the form of hydrates or by the addition of excess water, and then undergo hydrolysis through the loss of a proton by one or more of the water molecules. Subsequently, condensation takes place, generating metal-oxygen-metal (M–O–M) bridges for metal-oxide frameworks. When AcAc is involved as a fuel, it should be present in the vicinity of metal nitrates in the dried films to induce vigorous combustion between the oxidizer (metal nitrate) and the fuel during the subsequent annealing. AcAc also strongly tends to form a

chemical complex with metal cations. Free AcAcs, which do not chemically interact with the metal cations, do not take part in the combustion reaction, instead acting as impurities that have an adverse influence on device performance. In those reactions, the coordination number of the metal cations and the competitive formation of complexes by water molecules and AcAc are critically dependent on the environmental pH around the metal cations. Therefore, for multi-component combustion reactions, it is critical to control the chemical composition of the precursor solution: metal nitrate, AcAc, water, and pH-controlling acid or base. In addition, both the acid and base can stimulate the hydrolysis and condensation reaction; thus, the presence of these reactants makes the chemical reaction much more complicated.

In contrast, a strong exothermic reaction can also be initiated *via* combustion of the acetylacetonate complex, triggered by nitrate ions (Scheme 1). That is, acetylacetonate (fuel) and nitrate (oxidizer) ligands can serve as reactants in the combustion reaction of the IZO precursors. The exothermic heat generated by self-combustion of a fuel–oxidizer precursor pair can be used to form the corresponding oxides without applying a high annealing temperature. The use of fuel and oxidizer ligands eliminates the need for other chemical additives, which greatly simplifies the combustion-derived synthesis and improves its reproducibility. The ligands for either oxidizer or fuel are incorporated in stoichiometric ratios with regard to the metal precursors, so that their number is not altered during the combustion reaction. Water molecules may be associated with the precursors in the form of hydrates; the amount of associated water can be easily and accurately detected by thermogravimetric analysis. Therefore, the only variable that must be controlled is merely the relative composition of metal precursors, the influence of which can be monitored systematically through chemical analysis of the corresponding metal oxide skeletons and in-depth

investigation of device performance.

To investigate the spontaneous exothermic reaction of the fuel-oxidizer pair, thermogravimetric analysis (TGA) and differential thermal analysis (DTA) were conducted on various IZO precursors that were prepared using different combinations of In and Zn precursors (Fig. 2). A pair of In and Zn precursors containing acetylacetonate (fuel) and nitrate (oxidizer) ligands yielded films that clearly exhibited different thermal behavior compared to those from other pairs of In and Zn precursors, showing abrupt thermal decomposition around 200 °C. $I_{AC}Z_{AC}O$ and $I_{Cl}Z_{Cl}O$, which were not fuel–oxidizer combinations, underwent conventional condensation and showed small and broad endothermic peaks in the DTA thermogram in the temperature range of 100 – 300 °C, possibly due to the decomposition of organic ligands and the hydrolysis of the precursors. In addition, small exothermic peaks involving significant mass loss in the range of 250 – 500 °C could be explained by dehydroxylation, polycondensation, and pyrolysis of the organic components.[28,29] These results meant that the conventional IZO precursors required a high temperature of over 400 °C for complete conversion into the M–O–M lattice. The nitrate-based precursor of $I_{NO}Z_{NO}O$, another conventional precursor, showed two remarkable exothermic peaks at 120 and 350 °C with corresponding mass loss in two steps. The initial ~30% mass loss at the lower temperature could have originated from dehydration of water coordinated with the metal nitrate.[22] The second mass loss may have resulted from decomposition of anhydrous nitrate and the conversion of metal hydroxide to metal oxide *via* condensation. Therefore, nitrate-based precursors can be regarded as suitable candidates for TFT materials requiring a moderately high annealing temperature of ~400 °C despite their conventional processability.

On the other hand, an extremely intense exothermic peak at 200 °C was observed in the

$I_{NO}Z_{AC}O$ precursor and was attributed to the combustion process, with a corresponding tremendous loss in mass in the TGA thermogram, as shown in Fig. 2(a). The very fast and vigorous chemical reaction, indicated by a single narrow exothermic peak and abrupt mass loss, may provide supplemental energy to drive the formation of the M–O–M lattice and the removal of the organic ligands. From the thermal behavior of the In–Zn precursors, the decomposition and condensation temperature of the $I_{NO}Z_{AC}O$ precursor was found to be lower than that of other precursors, due to the heat supplied by the exothermic reaction. The precursors are listed in decreasing order of decomposition temperature as follows: $I_{NO}Z_{AC}O$ > $I_{NO}Z_{NO}O$ > $I_{AC}Z_{AC}O$ > $I_{Cl}Z_{Cl}O$. Such an exothermic reaction is expected to have a significant influence on the performance of IZO TFTs fabricated with low-temperature annealing.

To verify the chemical and structural composition of the IZO thin films, X-ray photoelectron spectroscopy (XPS) was performed. Fig. 3 and Supplementary Information Fig. S2† show the O 1s XPS spectra of the IZO thin films prepared with different combinations and composition ratios of In and Zn precursors. An asymmetric O 1s peak was consistently fitted to three different components centered at 529 ± 0.3 eV, 530.6 ± 0.3 eV, and 531.7 ± 0.3 eV, respectively, using Gaussian and Lorentzian functions. It was clear that the low binding energy at 529 ± 0.3 eV was caused by the O^{2-} ions, which were surrounded by In and Zn atoms. The middle binding energy at 530.6 ± 0.3 eV was closely related to the O^{2-} ions in the oxygen-deficient region. The high binding energy at 531.7 ± 0.3 eV was attributed to loosely bound hydroxyl groups (M–OH), which were caused by the absorbed H_2O, O_2, or OH species on the surface of the IZO thin films.[7,11,30-32] The IZO films from $I_{NO}Z_{AC}O$ prepared by the combustion process and those from $I_{AC}Z_{AC}O$, $I_{NO}Z_{NO}O$, and $I_{Cl}Z_{Cl}O$ prepared by the conventional process showed significant differences in the relative intensity of the three

different components in the O 1s peak. In particular, a large amount of M–O–M oxygen was observed in the $I_{NO}Z_{AC}O$ thin film in contrast to $I_{AC}Z_{AC}O$, $I_{NO}Z_{NO}O$, and $I_{Cl}Z_{Cl}O$. From a comparison with the other two peaks that appeared at 530 – 532 eV, we also estimated that $I_{NO}Z_{AC}O$ possessed a larger concentration of oxygen vacancies and minimal hydroxyl group content. A dispersed vacant state with short interaction distances should induce a minimum conduction band for efficient carrier transport, which can be achieved in metal oxide lattices but not in hydroxide lattices. Thus, M–O–M formation is an essential requirement for achieving high electrical performance from the amorphous metal oxide films. Generally, annealing temperature is critical to the TFT performance of solution-processed metal oxide semiconductors because the formation of the M–O–M lattice is driven by thermal condensation and dehydroxylation. Therefore, the degree of oxide lattice formation and oxygen vacancy generation primarily depends on the external thermal energy. From the XPS data, it can be inferred that the internal energy generated from the combustion of $I_{NO}Z_{AC}O$ largely contributed to the formation of M–O–M bonds and the suppression of M–OH bonds. Moreover, it is worth noting that the $I_{NO}Z_{AC}O$ thin films prepared at an annealing temperature of 300 °C showed a larger amount of M–O–M oxygen than the thin films from other conventional IZO precursors that were annealed at 350 °C, as shown in Supplementary Information Fig. S2†.

The composition ratio of the combustive In_{NO} and Zn_{AC} precursors in the $I_{NO}Z_{AC}O$ thin films also affected the relative intensity of three different components in the O 1s peak, as shown in Supplementary Information Fig. S3†. The dependence of the O 1s peak intensity on the composition of In_{NO} and Zn_{AC} can be explained in terms of the relative ratio between the fuel and the oxidizer. For example, when the content of fuel (Zn_{AC}) is higher than that of the

oxidizer (In_{NO}) or vice versa, the combustion process may not proceed to completion, resulting in a reduced M–O–M and an increased M–OH composition. In other words, an equivalent amount of fuel and oxidizer is required to create the proper combustion reaction. This explanation is also supported by the thermal behavior of the $I_{NO}Z_{AC}O$ prepared from In_{NO}/Zn_{AC} = 1:5, which exhibits relatively small exothermic peaks at a much higher temperature than where the peaks of In_{NO}/Zn_{AC} = 3:3 appear, as shown in Supplementary Information Fig. S5†. To verify further the influence of the fuel/oxidizer composition ratio on the electrical properties of IZO TFTs, $I_{AC}Z_{NO}O$ TFTs were fabricated from different ratios of In_{AC} and Zn_{NO} precursors. The electrical performance of $I_{AC}Z_{NO}O$ TFTs does in fact depend on the ratio of In_{AC} to Zn_{NO}, as shown in Supplementary Information Fig. S9†. Interestingly, in the case where the amount of In precursor is much higher than that of the Zn precursor, namely I_{AC}/Z_{NO} = 5:1, the electrical performance of the fabricated TFT was poor, with a low on/off current ratio and low mobility. This result can be attributed to the imbalance between the content of fuel (coordinated with In) and the content of oxidizer (coordinated with Zn). These results indicate that an equivalent amount of fuel and oxidizer is necessary to realize high field effect mobilities and high on/off current ratios from $I_{NO}Z_{AC}O$ and $I_{AC}Z_{NO}O$ TFTs fabricated with this process. The IZO thin films' chemical composition and structural characteristics, dependent on the ratio of In and Zn precursors, determined the electrical performance of the corresponding IZO TFTs, which will be discussed below.

The surface morphology and roughness of the IZO thin films prepared from different In and Zn precursors were investigated by atomic force microscopy (AFM) and field emission scanning electron microscopy (FE-SEM), as shown in Supplementary Information Fig. S6†. The IZO thin films from In_{NO} and Zn_{AC} precursors showed nanocrystalline structure whose

features were uniformly distributed and densely packed, compared to the relatively small nanocrystallites on the In_{NO}–Zn_{NO} thin films observed in the AFM surface images. Films prepared from In_{AC}–Zn_{AC} did not form nanocrystals, while those prepared from In_{Cl}–Zn_{Cl} yielded large rough agglomerates with a size of around 200 nm. Although it was nearly impossible to obtain the exact structural information on these nanocrystallites, we estimated that they developed during precursor condensation and became embedded in the overall amorphous IZO film structure, which was characterized using X-ray diffraction (XRD) as shown in Supplementary Information Fig. S8†. SEM imaging of the In_{AC}–Zn_{AC} thin films also revealed the existence of numerous pores on the surface, even though the surface appeared quite smooth when examined by AFM. The film thickness was derived from cross-sectional SEM images of the IZO thin films, which were sliced *via* ion milling. All IZO films had a thickness of approximately 8 nm.

IZO TFTs with a bottom-gate, top-contact structure were fabricated from spin-coated IZO channels on SiO_2 dielectrics after annealing at 350 °C in air. Al source–drain electrodes of 100 nm were subsequently deposited on IZO channel layers. All of the IZO TFTs operated properly as n-channel enhancement-mode devices and exhibited clear pinch-off and good current saturation, as shown in Fig. 4 and 5. All of the transistor parameters, such as mobility, threshold voltage, and on/off current ratio, are summarized in Table 1.

The electrical performance of the $I_{NO}Z_{AC}O$ TFTs was compared with other conventional IZO TFTs to investigate the influence of combustion chemistry on TFT properties, as shown in Fig. 4. The electrical performance of the $I_{NO}Z_{AC}O$ TFTs fabricated *via* combustion was significantly better than that of the other IZO TFTs, showing a much higher average field-effect mobility of 8.70 $cm^2 V^{-1} s^{-1}$ and an enhanced on/off current ratio of 1.06×10^8. The

electrical performance of the $I_{NO}Z_{AC}O$ TFTs was also significantly better than that of a-Si:H TFTs. The influence of annealing temperature on the electrical performance of the $I_{NO}Z_{AC}O$ TFTs is shown in Table 1 and Supplementary Information Fig. S10†. Increasing the annealing temperature from 250 to 350 °C raises the carrier mobility for $I_{NO}Z_{AC}O$ TFTs above that of typical solution-processed IZO TFTs (Table 1). The $I_{NO}Z_{AC}O$ TFTs fabricated at low temperature of 250 °C exhibited reasonable electrical performance, even though the combustion reaction did take place at a low temperature of around 200 °C. For complete formation of the M–O–M bonds, we believe that a minimum of 300 °C of external thermal energy is required, even though the heat generated from the combustion reaction can provide additional energy for the metal oxide formation. This energy requirement can be verified by the additional increase in the M–O–M XPS peak intensity as the annealing temperature is increased from 250 to 350 °C (Supplementary Information Fig. S2†). An annealing temperature of 300 °C is compatible with flexible substrates, such as polyimide or PAR films. The $I_{NO}Z_{AC}O$ TFTs prepared at 300 °C exhibited a good average field-effect mobility of 3.67 $cm^2 V^{-1} s^{-1}$ and an on/off current ratio of 2.57×10^7, with a slight display of hysteresis.

The transfer and output characteristics of the $I_{NO}Z_{AC}O$ TFTs prepared from various composition ratios of In_{NO} to Zn_{AC} precursors were investigated to establish the optimal composition for high TFT electrical performance (Fig. 5). The IZO TFTs fabricated *via* the self-combustion of coordinated fuel and oxidizer ligands at an annealing temperature of 350 °C showed excellent TFT properties with negligible electrical hysteresis. The average saturation mobilities corresponding to various In_{NO} and Zn_{AC} composition ratios were in the range of 0.31 – 8.70 $cm^2 V^{-1} s^{-1}$ with an on/off current ratio of 10^4 – 10^8. Interestingly, when the Zn/In ratio was 2:1, the electrical performance of the IZO TFTs was particularly poor,

which was ascribed to a reduction in charge carriers due to the decrease in In content. Generally, the addition of In^{3+} can create more oxygen vacancies, which can accelerate electron mobility throughout the amorphous structure of the IZO thin film, where the In–O bond strength is weaker than that of the Zn–O bond owing to the difference in electronegativity between In and Zn.[33-35] It has also been reported that extensive overlap between neighboring s orbitals of In^{3+}, which are larger than those of Zn^{2+}, may improve the electrical conductivity of IZO thin films.[36] Therefore, it is natural that the $I_{NO}Z_{AC}O$ TFTs with higher In content exhibited better electrical properties than $I_{NO}Z_{AC}O$ TFTs containing higher Zn content. Nevertheless, the $I_{NO}Z_{AC}O$ TFTs a stoichiometric ratio of In and Zn exhibited the best field effect mobility with the highest on/off current ratio. This particular electrical performance could be ascribed to the high condensation efficiency from the effective combustion reaction where the amounts of fuel and oxidizer were equivalent. These results also correspond well to the XPS data that show an extremely large M–O–M peak in the IZO thin film with a composition ratio of $In_{NO}/Zn_{AC} = 3:3$.

Device uniformity is of substantial importance for the practical use of TFTs. To measure the uniformity of the $I_{NO}Z_{AC}O$ TFTs, 30 TFT units were fabricated at an annealing temperature of 350 °C. The performance of TFT units was measured, and standard deviations were obtained for the mobility (μ = 8.70 ± 1.75 $cm^2 V^{-1} s^{-1}$) and the turn-on voltage (V_{ON} = 12.47 ± 2.68 V) (Fig. 6). This result demonstrates that the $I_{NO}Z_{AC}O$ TFTs exhibit good device uniformity and reproducible yield. A very high mobility (13.8 $cm^2 V^{-1} s^{-1}$) was observed in some of the devices suggesting that the device performance can be further improved by optimizing the processing conditions.

The precursor solutions prepared in our study were also applied towards the inkjet

printing of TFTs. A solution of $I_{NO}Z_{AC}O$ with an identical composition ratio of In and Zn was inkjet-printed and annealed at 350 °C; the resulting film was then incorporated into a TFT. The transfer and output characteristics of the inkjet-printed $I_{NO}Z_{AC}O$ TFT are shown in Supplementary Information Fig. S11†. The saturation mobility was 5.3 $cm^2 V^{-1} s^{-1}$, and the on/off current ratio was 10^6. This result demonstrates that a high performance IZO TFT can be fabricated by inkjet printing without photolithography or vacuum-based techniques.

3. Conclusions

We have demonstrated that IZO thin films suitable for TFTs can be fabricated by the self-combustion of a two-component mixture of metal salts whose ligands function both as a fuel and as an oxidizer. The properties of the IZO TFTs depended on the precursor composition and annealing temperature. TFTs fabricated using the self-combustion system demonstrated high reproducibility and device uniformity, compared to those fabricated *via* previously reported general combustion of multi-component systems. The combustion of In and Zn precursors containing acetylacetonate (fuel) and nitrate (oxidizer) can release extremely intense exothermic heat, and this evolution of internal energy can be utilized to lower the externally applied temperature for annealing of the oxide precursors. Our results confirmed that the energy from the combustion reaction can facilitate the formation of the M–O–M lattice and the removal of organic ligands, inducing higher carrier mobility in IZO TFTs. Furthermore, the precursor composition had a remarkable effect on the chemical and electrical characteristics of the IZO thin films. The IZO TFTs prepared by using an equivalent stoichiometric ratio of fuel and oxidizer at an annealing temperature of 350 °C showed

superior field-effect mobility of 13.8 $cm^2 V^{-1} s^{-1}$, and an on/off current ratio of 1.06×10^8. IZO TFTs fabricated by inkjet printing of the precursor mixture, followed by annealing at 350 °C, exhibited a high mobility of 5.3 $cm^2 V^{-1} s^{-1}$ with an on/off ratio of 10^6. Such high TFT performance at low processing temperature, with good device uniformity and high yield, demonstrate the potential for application of the proposed system in flexible printed electronics. An additional advantage that should be emphasized is that our system allows high-quality solution-processed semiconductor films to be prepared from a simple mixture of two oxide precursors without any additives. Application of our self-combustion method to the synthesis of ternary oxide films is under investigation.

4. Experimental section

Preparation of the IGO precursor solutions (General Combustion with Additives)

All reagents, indium nitrate hydrate ($In(NO_3)_3 \cdot H_2O$, 99.99%), gallium nitrate hydrate ($Ga(NO_3)_3 \cdot H_2O$, 99.9%), monoethanolamine ($NH_2CH_2CH_2OH$, 99%), acetylacetone (AcAc, $CH_3COCH_2COCH_3$, 99%), ammonium hydroxide solution (NH_4OH, 28% in water), and 2-methoxyethanol ($CH_3OCH_2CH_2OH$, anhydrous 99.8%), were purchased from Aldrich and used without additional purification. General precursor solutions, without the fuel and oxidizer for the combustion reaction, were first prepared in order to optimize the ratio of metal ions. 0.2 M metal salt precursor solutions were prepared in 2-methoxyethanol (99%) with monoethanolamine (99%) as a stabilizer. The molar ratios of In:Ga in the precursor solutions were 100:0, 94:6, 88:12, and 76:24. The prepared clear solutions were stirred for 3 h at room temperature prior to spin-coating. The precursor solutions for inducing the combustion reaction were prepared as follows. Metal salt precursors with a concentration of

0.2 M (In nitrate : Ga nitrate = 94:6 molar ratio) were dissolved in 2-methoxyethanol with the appropriate amount of AcAc, and an ammonium hydroxide solution was subsequently added gently with stirring. The composition of AcAc was varied over a range of R_1 values from 1 to 3, where R_1 indicates the molar ratio of AcAc to metal salts. The composition of ammonium hydroxide solution was varied over a range of R_2 values from 1 to 4, where R_2 indicates the molar ratio of water molecule in an ammonium hydroxide solution to metal salts. The clear solutions were stirred for 12 h at room temperature prior to spin coating.

Preparation of the IZO precursor solutions (Additive-Free Self-Combustion)

The IZO precursor solutions were prepared using zinc acetylacetonate hydrate ($Zn(C_5H_7O_2)_2{\cdot}xH_2O$), zinc nitrate hexahydrate ($Zn(NO_3)_2{\cdot}6H_2O$), zinc chloride ($ZnCl_2$), indium acetylacetonate ($In(C_5H_7O_2)_3{\cdot}xH_2O$), indium nitrate hydrate ($In(NO_3)_3{\cdot}xH_2O$), and indium chloride ($InCl_3$), which were all obtained from Sigma-Aldrich. After the metal salts were dissolved in anhydrous 2-methoxyethanol (Aldrich), the solutions were thoroughly stirred for more than 6 h at room temperature to prepare the homogeneous precursor solution. The total concentration of the IZO precursor was fixed at 0.1 M, and the molar ratio of indium nitrate hydrate to zinc acetylacetonate hydrate was varied in the range of 1:5 – 5:1 to determine the optimal composition. Various In and Zn precursors were combined at a fixed molar concentration of 0.05 M:0.05 M to compare the thermal behavior and TFT properties of films prepared from the combustive IZO precursor solutions with those of the conventional IZO. Thermal behavior was observed in an ambient atmosphere *via* TGA and DTA (SDT 2060, TA Instruments, USA). The heating rate of TGA and DTA was 10 °C min^{-1}.The samples for thermal analysis were prepared by evaporating the $I_{NO}Z_{AC}O$, $I_{AC}Z_{AC}O$, $I_{NO}Z_{NO}O$, and $I_{Cl}Z_{Cl}O$

precursor solutions at 40 °C in a vacuum oven for 1 day.

Characterization of the IZO thin films

The microstructure of the IZO thin films was investigated by an ultra high resolution (UHR) FE-SEM (S-5500, Hitachi, Japan). The thickness of the IZO thin films was measured with the UHR FE-SEM after the cross-sectional samples were prepared in the following manner. Platinum thin films with a thickness of approximately 100 nm were deposited on the prepared IZO thin films with a coating machine (E-1030, Hitachi, Japan) to distinguish each layer. The IZO thin films were then cut with an ion milling system (E-3500, Hitachi, Japan) at a power level of 6 keV and a constant Ar flow rate of 50 sccm. The fine surface roughness of the IZO thin films was explored by AFM (NanoScope, Veeco, USA) in an area of 3μm^2 *via* noncontact mode. The IZO thin films produced after annealing at 350 °C were analyzed *via* XRD (D-MAX-RC, Rigaku, Japan). XRD measurements were performed using a thin film diffractometer in which samples were fixed at an angle of 3° to the X-ray beam with 2θ scan of the detector. The source power was 60 mA/40 kV, which was stronger than that for normal powder XRD. An X-ray photoelectron spectrometer (K-Alpha, Thermo Fisher Scientific, USA), with an Al Kα excitation source, was used to characterize the surface chemical composition and the chemical state of the IZO thin films. All XPS spectra were calibrated against the C 1s electron peak at 286.5 eV.

Fabrication and electrical measurement of IZO TFTs

A bottom-gate, top-contact design was adopted in for the IZO TFTs as a typical device structure. The IZO precursor solutions were deposited on a 300-nm thick SiO_2 film on a Si

wafer (heavily n-type doped) using a simple spin-coating method. Prior to deposition, the substrate was consecutively cleaned by consecutive treatments of ultrasonication in a detergent solution, acetone, and hot isopropyl alcohol. The SiO_2 substrate was then dried and treated with an ozone plasma for 20 min. The IZO precursor solutions were spin-coated at 4000 rpm for 30 s and pre-baked on a hot plate at 100 °C for 10 min to remove residual solvent and organic materials. After the pre-baking, the IZO thin films were annealed at 350 °C for 1 h on a hot plate in ambient air. The top-contact source and drain electrodes (100 nm thickness, Al) were thermally evaporated through a patterned metal shadow mask. The ratio of the channel width and channel length was 60 (width = 3000 μm; length = 50 μm). The inkjet printing was also carried out using piezoelectric inkjet nozzle with the orifice size of 30 μm (Microfab, USA).

The IZO ink for inkjet printing consisted of the In and Zn precursors in a ratio identical to the optimal composition for the spin-coated films. The inkjet printing was carried out at 25 °C using a piezoelectric inkjet nozzle with an orifice size of 30 μm (Microfab, USA) operated at a head frequency of 200 Hz and a resolution of 500 DPI. Pre-baking and annealing was conducted in the manner described above.

The electrical characteristics of the IZO TFTs were measured in air using a semiconductor parameter analyzer (4155C, Agilent, USA). The measurements were typically taken in continuous mode, and the transfer curve was recorded before the output curve. The field-effect mobility (μ_{sat}) and the threshold voltage (V_{th}) were calculated for the saturation region *via* Equation 1,

$$I_D = \mu_{sat} C_i \frac{W}{2L} (V_G - V_{th})^2, \quad (1)$$

where I_D is the saturation current, C_i is the capacitance per unit area of the dielectric, V_G is the source-gate voltage, and W and L are the TFT channel width and length, respectively.

Acknowledgements

This work was supported by a grant from R&D Convergence Program of Ministry of Science, ICT, and Future Planning and Korea Research Council for Industrial Science and Technology of Republic of Korea (Grant B551179-09-06-00). We would like to thank Dr. T.-S. Bae (UHR FE-SEM group, Korea Basic Science Institute, Jeonju) for assistance with the SEM imaging.

References

1 K. Nomura, H. Ohta, K. Ueda, T, Kamiya, M. Hirano, H. Hosono, *Science,* 2003, **30**, 1269-1272.

2 O. Nilsen, R. Balasundaraprabhu, E. V. Monakhov, N. Muthukumarasamy, H. Fjellvag, B. G. Svensson, *Thin Solid Films,* 2009, **517**, 6320-6322.

3 Y. Vygranenko, K. Wang, A. Nathan, *Appl. Phys. Lett.,* 2007, **91**, 263508.

4 J. S. Park, K. S. Kim, Y. G. Park, Y. G. Mo, H. D. Kim, J. K. Jeong, *Adv. Mater.,* 2009, **21**, 329-333.

5 J. H. Cho, J. Lee, Y. He, B. Kim, T. P. Lodge, C. D. Frisbie, *Adv. Mater.,* 2008, **20**, 686-690.

6 J. W. Hennek, Y. Xia, M. C. Hersam, A. Facchetti, T. J. Marks, *ACS Appl. Mater. Interfaces,* 2012, **4**, 1614-1619.

7 S. Y. Cho, Y. H. Kang, J. Y. Jung, S. Y. Nam, J. Lim, S. C. Yoon, D. H. Choi, C. Lee, *Chem. Mater.,* 2012, **24**, 3517-3524.

8 E. Fortunato, P. Barquinha, R. Martins, *Adv. Mater.,* 2012, **24**, 2945-2986.

9 K. Song, J. Noh, T. Jun, Y. Jung, H. Kang, J. Moon, *Adv. Mater.,* 2010, **22**, 4308-4312.

10 H. S. Kim, P. D. Byrne, A. Facchetti, T. J. Marks, *J. Am. Chem. Soc.,* 2008, **130**, 12580-12581.

11 W. K. Lin, K. C. Liu, S. T. Chang, C. S. Li, *Thin Solid Films,* 2012, **520**, 3079-3083.

12 S. Hwang, J. H. Lee, C. H. Woo, J. Y. Lee, H. K. Cho, *Thin Solid Films,* 2011, **519**, 5146-5149.

13 J. W. Hennek, M. G. Kim, M. G. Kanatzids, A. Facchetti, T. J. Marks, *J. Am. Chem. Soc.,* 2012, **134**, 9593-9596.

14 D. H. Lee, S. Y. Han, G. S. Herman, C. Chang, *J. Mater. Chem.,* 2009, **19**, 3135-3137.

15 M. G. Kim, H. S. Kim, Y. G. Ha, J. Q. He, M .G. Kanatzidis, A. Facchetti, T. J. Marks, *J. Am. Chem. Soc.,* 2010, **132**, 10352-10364.

16 S. Y. Han, G. S. Herman, C. Chang, *J. Am. Chem. Soc.,* 2011, **133**, 5166-5169.

17 K. K. Banger, Y. Yamashita, K. Mori, R. L. Peterson, T. Leedham, J. Rickard, H. Sirringhaus, *Nat. Mater.,*2011, **10**, 45-50.

18 Y. H. Kim, J. S. Heo, T. H. Kim, S. Park, M. H. Yoon, J. Kim, M. S. Oh, G. R. Yi, Y. Y. Noh, S. K. Park, *Nat. Lett.,*2012, **489**, 128-132.

19 M. G. Kim, M. G. Kanatzids, A. Facchetti, T. J. Marks, *Nat. Mater.,* 2011, **10**, 382-388.

20 M. G. Kim, J. W. Hennek, H. S. Kim, M. G. Kanatzids, A. Facchetti, T. J. Marks, *J. Am. Chem. Soc.,* 2012, **134**, 11583-11593.

21 Z. Yue, J. Zhou, L. Li, H. Zhang, Z. Gui, *J. Magn.Magn.Mater*., 2000, **208**, 55-60.

22 S. Yuvaraj, F. Y. Lin, T. H. Chang, C. T. Yeh, *J. Phys. Chem. B,* 2003, **107**, 1044-1047.

23 C. –C. Hwang, T. –Y. Wu, J. Wan, J. –S. Tsai, *Mater. Sci. Eng. B,* 2004, **111**, 49-56.

24 M. Epifani, E. Melissno, G. Pace, M. Schioppa, *J. Euro. Cerm. Soc.,* 2007, **27**, 115-123.

25 S. Music, A. Saric, S. Popovic, *Ceram. Int.,* 2010, **36**, 1117-1123.

26 S. Esposito, M. Turco, G. Bangasco, C. Cammarano, P. Pernice, A. Aronnc, *Appl. Catal., A: Gen.,* 2010, **372**, 48-57.

27 D. Visinescu, B. Jurca, A. Ianculescu, O. Carp, *Polyhedron*, 2011, **30**, 2824-2831.

28 G. H. Kim, B. D. Ahn, H. S. Shin, W. H. Jeong, H. J. Kim, H. J. Kim, *Appl. Phys. Lett.,* 2009, **94**, 233501.

29 D. H. Yoon, S. J. Kim, W. H. Jeong, D. L. Kim, Y. S. Rim, H. J. Kim, *J. Cryst. Growth,* 2011, **326**, 171-174.

30 S. Jeong, Y. G. Ha, J. Moon, A. Facchetti, T. J. Marks, *Adv. Mater.,* 2010, **22**, 1346-1350.

31 Y. S. Rim, W. H. Jeong, D. L. Kim, H. S. Lim, K. M. Kim, H. J. Kim, *J. Mater. Chem.,* 2012, **22**, 12491-12497.

32 T. Jun, Y. Jung, K. Song, J. Moon, *ACS Appl. Mater. Interfaces,* 2011, **3**, 774-781.

33 L. Lu, M. Echizen, T. Nishida, Y. Ishikawa, K. Uchiyama, Y. Uraoka, *AIP adv.,* 2012, **2**, 032111.

34 P. K. Nayak, T. Busani, E. Elamurugu, P. Barquinha, R. Martins, Y. Hong, E. Fortunato, *Appl. Phys. Lett.,* 2010, **97**, 183504.

35 D. N. Kim, D. L. Kim, G. H. Kim, S. J. Kim, Y. S. Rim, W. H. Jeong, H. J. Kim, *Appl. Phys. Lett.,* 2010, **97**, 192105.

36 C. Y. Koo, K. Song, T. Jun, D. Kim, Y. Jeong, S. H. Kim, J. Ha, J. Moon, *J. Electrochem. Soc.,* 2010, **157**, J111-J115.

The Table of Contents Entry

The self-combustion of In and Zn precursors coordinated with the fuel and oxidizer ligands is utilized for the high performance IZO TFTs.

Two-Component Solution Processing of Oxide Semiconductors for Thin-Film Transistors *via* Self-Combustion Reaction

Young Hun Kang,‡ Sunho Jeong,‡ Jung Min Ko, Ji-Yoon Lee, Youngmin Choi, Changjin Lee,* and Song Yun Cho*

ToC figure

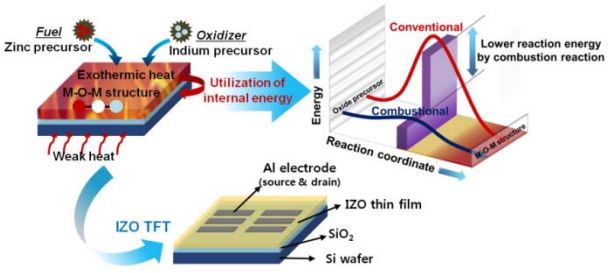

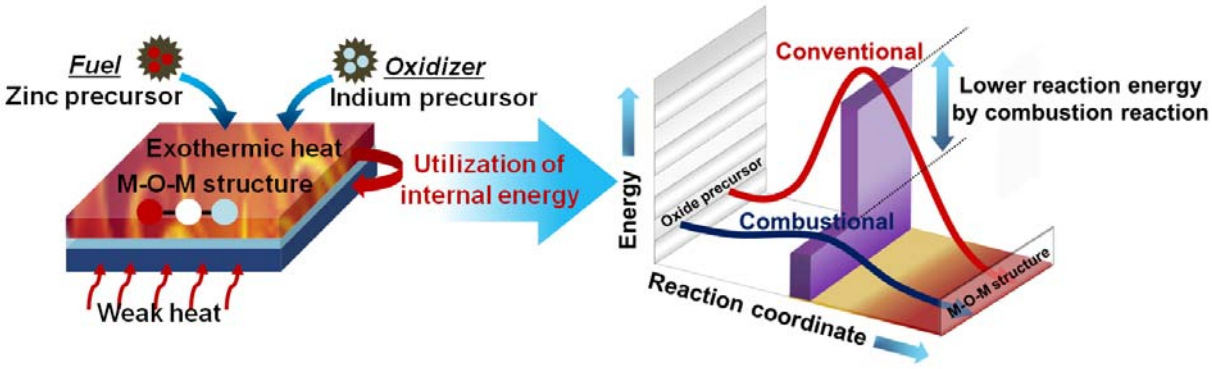

Scheme 1 A schematic diagram of the metal oxide film synthesis *via* self-combustion of metal precursors bearing coordinated fuel and oxidizer ligands.

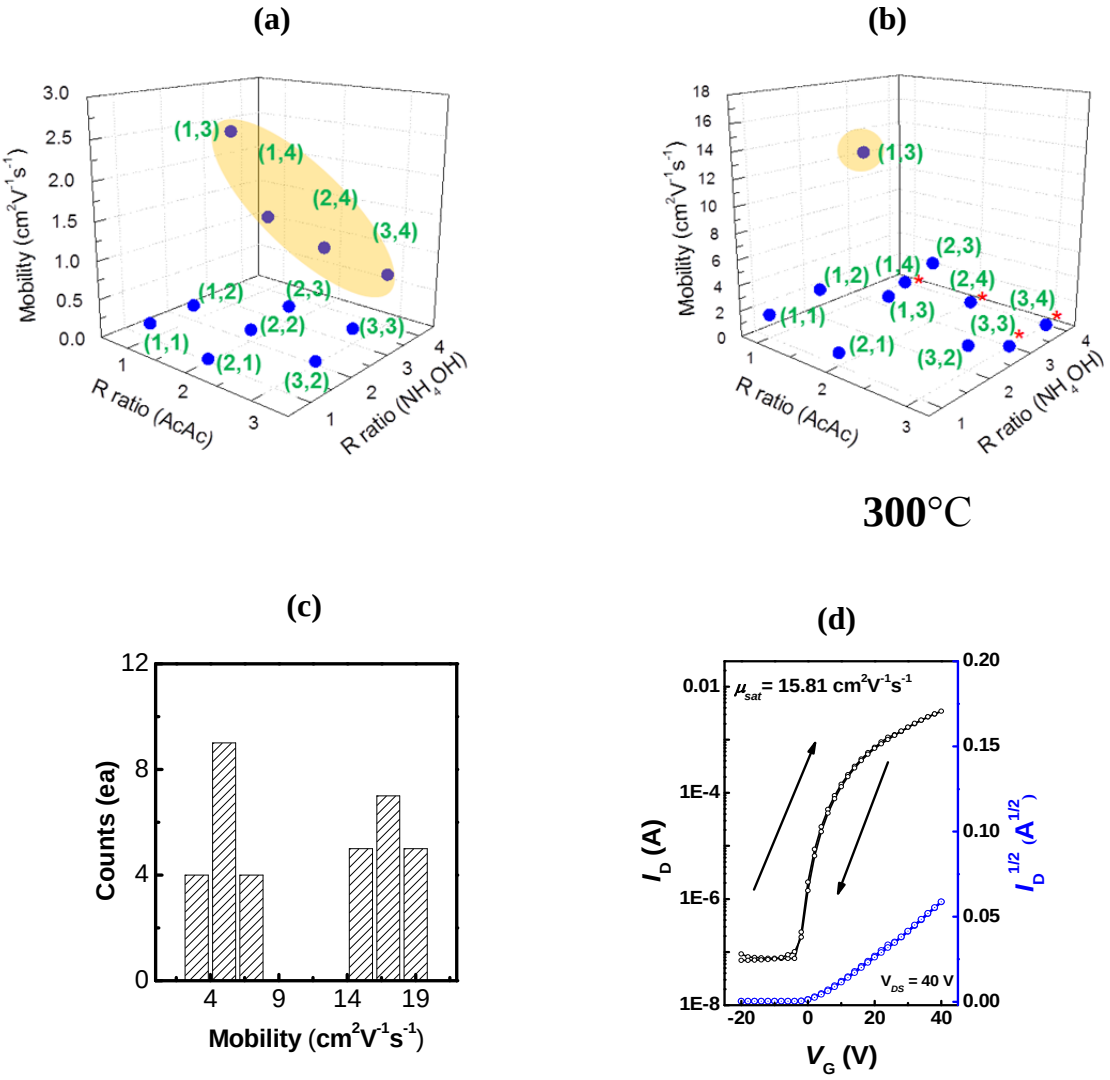

Fig. 1 Electrical performance of IGO TFTs, prepared *via* conventional chemical combustion with added fuel (AcAc) and NH_4OH. The TFT performance depends on the ratio of AcAc and NH_4OH at annealing temperature of (a) 250 and (b) 300°C. R_1 indicates the molar ratio of AcAc to metal salts. R_2 indicates the molar ratio of water molecule in an ammonium hydroxide solution to metal salts, respectively. (c) Device uniformity of IGO TFTs prepared from the IGO precursor with a composition ratio of AcAc/NH_4OH = 1/3 at 300°C. (d) A representative transfer curve for an IGO TFT.

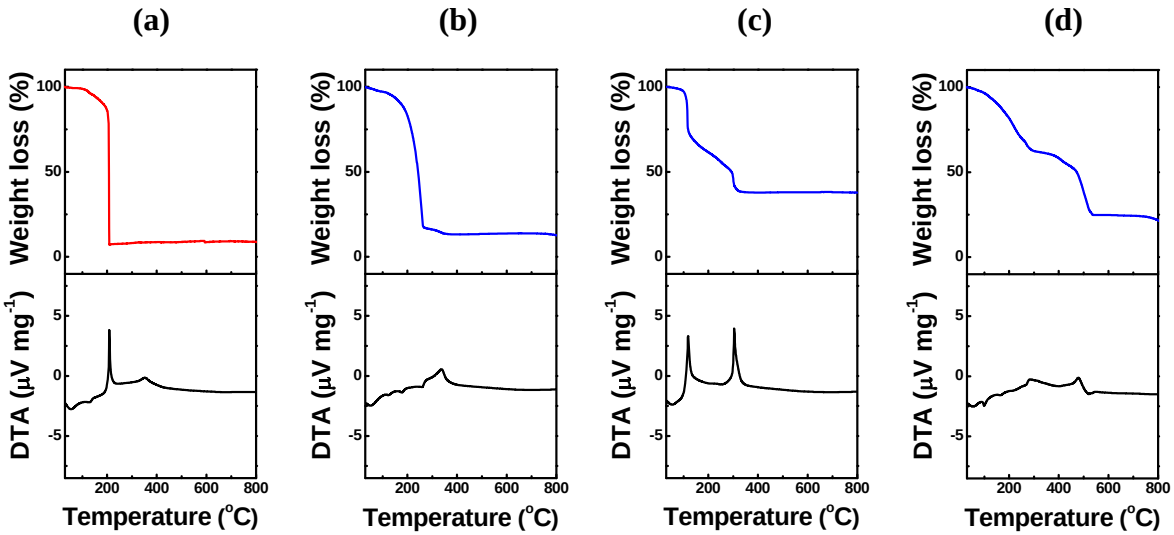

Fig. 2 Thermal behavior of IZO precursors prepared from various In and Zn precursors: (a) $I_{NO}Z_{AC}O$, (b) $I_{AC}Z_{AC}O$, (c) $I_{NO}Z_{NO}O$, and (d) $I_{Cl}Z_{Cl}O$.

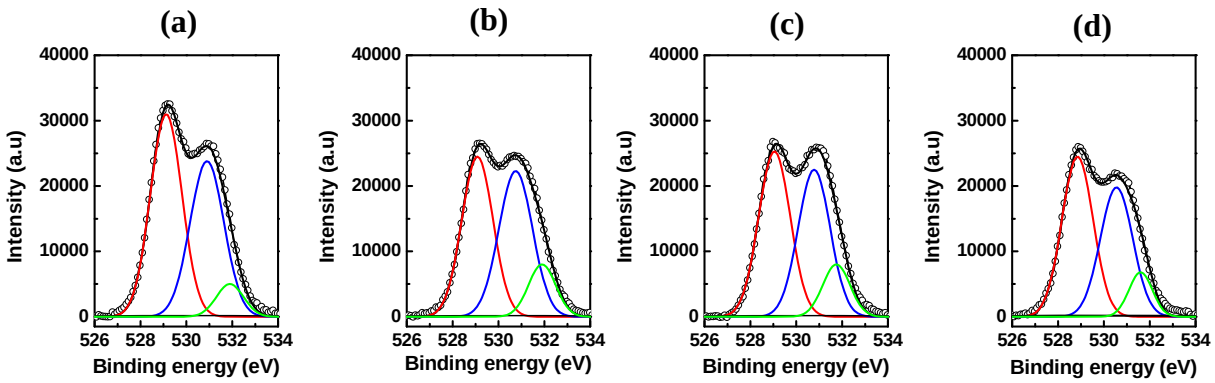

Fig. 3 XPS spectra of IZO thin films prepared from various In–Zn precursor pairs after annealing at 350°C: (a) $I_{NO}Z_{AC}O$, (b) $I_{AC}Z_{AC}O$, (c) $I_{NO}Z_{NO}O$, and (d) $I_{Cl}Z_{Cl}O$.

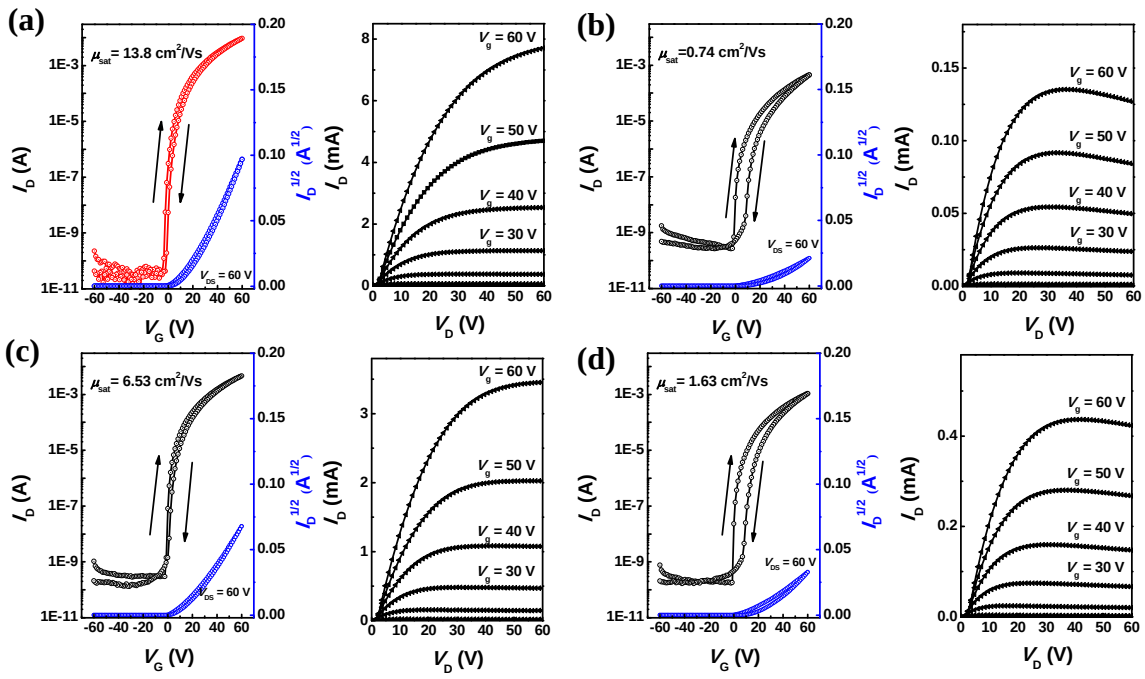

Fig. 4 The transfer and output characteristics of IZO TFTs fabricated from different In and Zn precursors: (a) $I_{NO}Z_{AC}O$, (b) $I_{AC}Z_{AC}O$, (c) $I_{NO}Z_{NO}O$, and (d) $I_{Cl}Z_{Cl}O$.

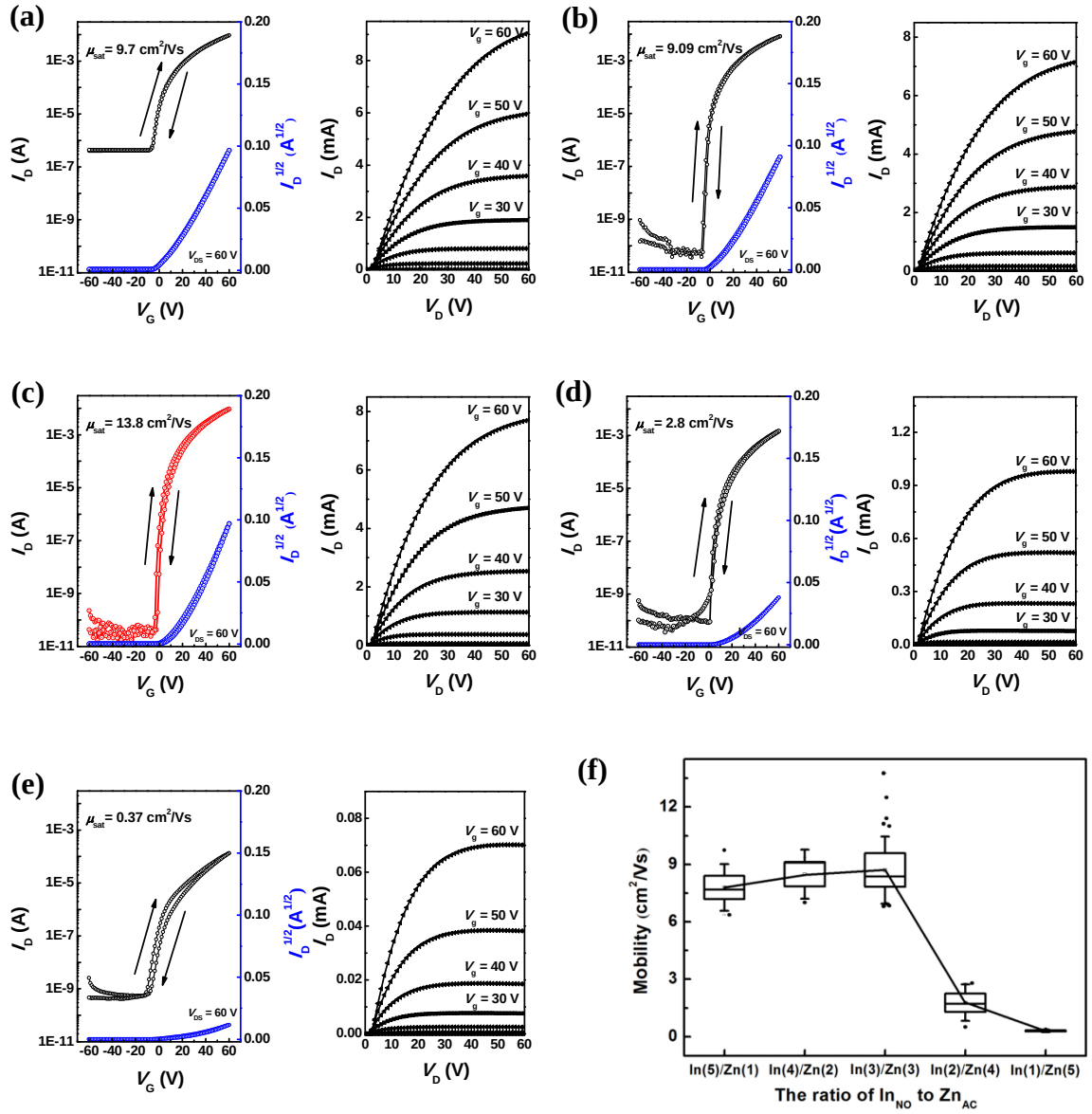

Fig. 5 The transfer and output characteristics of $I_{NO}Z_{AC}O$ TFTs fabricated from precursors with different composition ratios of In_{NO} to Zn_{AC}: (a) In_{NO}/Zn_{AC} = 5/1, (b) In_{NO}/Zn_{AC} = 4/2, (c) In_{NO}/Zn_{AC} = 3/3, (d) In_{NO}/Zn_{AC} = 2/4, and (e) In_{NO}/Zn_{AC} = 1/5. (f) The average mobility of the $I_{NO}Z_{AC}O$ TFTs.

Table 1 The characteristics of the IZO TFTs according to the different combinations and compositions of In–Zn precursors at various annealing temperatures.

IZO precursor	Average mobility ($cm^2 V^{-1} s^{-1}$)	Maximum mobility ($cm^2 V^{-1} s^{-1}$)	Threshold voltage (V)	Sub-threshold slope (V)	On/Off ratio	Annealing temperature (°C)
$In_{NO}(3)–Zn_{AC}(3)$	8.70 ± 1.75	13.80	12.47 ± 2.68	7.2	1.06×10^8	350
$In_{AC}(3)–Zn_{AC}(3)$	0.72± 0.09	0.73	21.99 ± 4.18	9.6	1.18×10^6	350
$In_{NO}(3)–Zn_{NO}(3)$	6.20± 0.29	6.53	17.24 ± 3.65	10.8	3.55×10^7	350
$In_{Cl}(3)–Zn_{Cl}(3)$	1.61± 0.02	1.63	16.55 ± 0.37	9.6	3.93×10^7	350
$In_{NO}(5)–Zn_{AC}(1)$	7.79 ± 1.22	9.70	9.01 ± 1.18	8.4	4.48×10^4	350
$In_{NO}(4)–Zn_{AC}(2)$	8.49 ± 1.29	9.09	10.05 ± 1.93	8.4	2.31×10^8	350
$In_{NO}(2)–Zn_{AC}(4)$	1.78 ± 0.95	2.80	22.56 ± 1.09	9.6	3.31×10^8	350
$In_{NO}(1)–Zn_{AC}(5)$	0.31 ± 0.07	0.37	22.25 ± 5.93	16.8	2.62×10^7	350
$In_{NO}(3)–Zn_{AC}(3)$	1.17 ± 0.28	1.49	17.49 ± 4.93	13.2	2.62×10^6	250
$In_{NO}(3)–Zn_{AC}(3)$	3.67± 1.08	4.91	16.72 ± 3.85	12.2	2.57×10^7	300

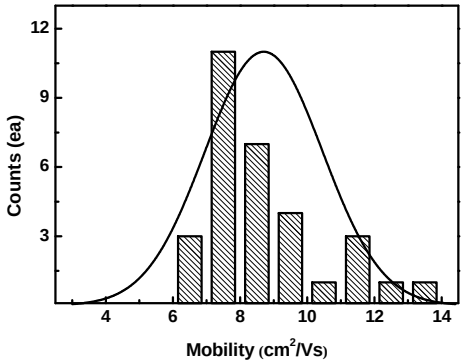

Fig. 6 Device uniformity of the $I_{NO}Z_{AC}O$ TFTs prepared from a precursor with a composition ratio of In_{NO}/Zn_{AC}=3/3.